Fermilab Library
0 1160 0038639 5

255

MIDWESTERN UNIVERSITIES RESEARCH ASSOCIATION

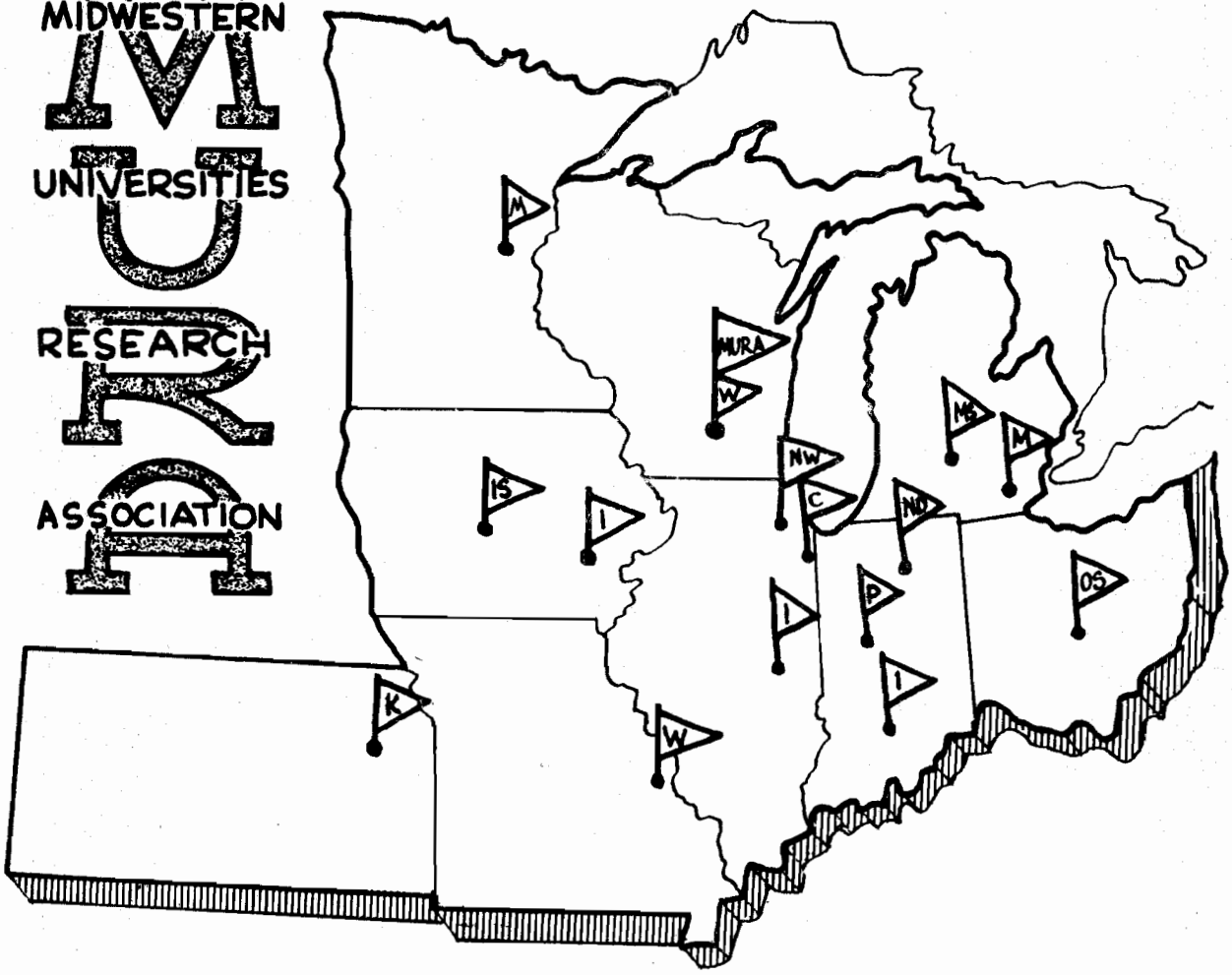

RADIO FREQUENCY EXPERIMENTS WITH AN FFAG ELECTRON MODEL ACCELERATOR

K. M. Terwilliger, L. W. Jones and C. H. Pruett

REPORT NUMBER 255

MIDWESTERN UNIVERSITIES RESEARCH ASSOCIATION*

2203 University Avenue, Madison, Wisconsin

RADIO FREQUENCY EXPERIMENTS WITH AN FFAG ELECTRON MODEL ACCELERATOR

K. M. Terwilliger**, L. W. Jones** and C. H. Pruett

April, 1957

ABSTRACT: Radio frequency experiments performed on the FFAG electron model accelerator demonstrate predictions of the Symon-Sessler rf acceleration theory. In particular the experiments show the phenomena of phase displacement in which a frequency modulated rf pulse, with frequency starting below that of a coasting beam, and sweeping through it, captures only a few particles and decreases the energy of the remainder a predictable amount. Measurements of the amount of average and peak energy loss of the coasting beam are in rough quantitative agreement with the theoretical predictions. Some qualitative tests are made which demonstrate beam stacking.

* Supported by Contract AEC #AT (11-1)-384

** On leave from University of Michigan

Introduction:

Symon and Sessler have proposed a theory of rf acceleration processes for FFAG accelerators.[1] A consequence of this theory is the possibility of obtaining large beam currents by a successive stacking procedure with repetitive rf cycles. To verify this rf acceleration theory, hereafter referred to as SS, a group of rf experiments have been performed on the the FFAG radial sector electron model.[2] Section A of this report gives a description of the methods used to perform the experiments, discussing the betatron and rf wave forms available. Section B presents the experiments and the results.

A. General description of experimental methods.

A magnetic field pulse through the betatron core can be used to accelerate the electrons from injection to an intermediate energy, where they can coast, not being accelerated. A second pulse can then accelerate them the remainder of the way to the target. Fig. 1 indicates this procedure, Fig. 1a showing the voltage from the betatron core as a function of time, and Fig. 1b the portion of this waveform actually used for acceleration; injection is indicated by a spike near the peak of the first pulse. Fig. 1c shows a photomultiplier pulse from the beam striking the target during the second betatron pulse. The coasting energy of the electrons can be easily varied by changing the time of injection with respect to the first betatron pulse. By varying the turn on time of the second betatron pulse, the beam half life due to gas scattering can be found. It is of order one millisecond at a pressure of 1×10^{-6} mm of Hg, so only a few milliseconds are available for rf experiments. The first betatron pulse has a tail, due to decay of eddy

[1] MURA-106

[2] MURA-219

currents in the betatron core, which accelerates the electrons appreciably out to about 2 milliseconds. Experiments on the coasting beam are performed after this period.

A system which provides frequency modulated rf pulses is described in detail in an accompanying report[3]. The required frequency modulation is obtained by voltage polarization of ferroelectric capacitors, which provides up to 10 Mc of frequency swing. The magnitude of the rf pulse, known from a calibrated peak reading voltmeter connected across the rf gap, is fairly constant over the high 5 Mc of the frequency range, and can have a value up to about 50 volts peak. Actually most of the rf experiments are done with a one to two Mc sweep. The turn on time of the rf pulse is one to two μsec, which is short compared to the typical phase oscillation period of about 30 μsec. The rf pulses can be repeated with less than 100 μsec spacing between them. The rf frequency as a function of time is measured by observing on an oscilliscope the beat of the frequency modulated rf signal with a constant frequency signal generator. The successive pulses repeat their fm cycles to within a few kc; the voltage patterns also reproduce fairly accurately. Fig. 2 shows some rf pulses and their beat frequency patterns. Fig. 4 is a frequency as a function of time curve obtained by the beat method. Over the frequency range covered the curve is accurately represented as $f = f_0(1 - e^{-\beta t})$ Both f_0 and β are easily varied parameters. Fig. 3 shows a case of a single rf pulse whose starting frequency is that of the coasting electrons, capturing a portion of the beam, and accelerating it to the target. The portion of the coasting not captured is accelerated to the target by the second betatron pulse. This second betatron pulse may be used as an energy analyzer of the electrons in the machine at the end of any rf manipulations.

[3] MURA-254

A quantity used a number of times in these experiments is df/dE, the change in electron revolution frequency per unit energy. This can be calculated, knowing the electron energy, but it is more accurate to measure this quantity directly, and then calculate the energy as discussed later. df/dE can be experimentally determined with the use of the second betatron pulse as follows. The energy difference between the coasting electrons and the target energy is simply the volts per turn times the number of turns the electrons are accelerated by the second betatron pulse, all measurable quantities. The coasting electron frequency is found by the rf oscillator, by finding the turn on frequency where the electrons are captured. The coasting energy of the electrons is then changed, by changing the time of injection, all other machine parameters being held constant. The new coasting beam-target energy difference is determined and the new coasting beam frequency found. These measurements give df/dE for the coasting beam.

The energy of the coasting electrons and the energy of the electrons as they hit the final target can be approximately determined from radius and field measurements. Fig. 5 shows calculated electron energy and revolution frequency as a function of radius, for a given set of magnet currents. It may be noted that in this accelerator the transition energy would be above 500 kev, so that in all cases of interest the energy and frequency both always increase with radius. A precise value of E is not needed in these experiments but it is interesting to see how well it can be determined. The calculated energy is not too accurate because of finite amplitudes of betatron oscillation and perturbations of the equilibrium orbit. These effects are important in FFAG accelerators because of the large field gradient and consequent rapid change of energy with radius. Accurate measurement of the electron

revolution frequency with the rf oscillator does not appreciably improve the energy determination. A quite accurate method of finding the energy is available however. In scaling FFAG accelerators, there is the following relation between parameters[1],

$$\frac{E}{f}\frac{df}{dE} = \frac{(k+1)E_0^2 - E^2}{(k+1)(E^2 - E_0^2)}$$

where k is the field index, f the particle revolution frequency, and E and E_0 the total and rest energies of the electron respectively. The quantities k, f and df/dE are experimentally measurable, so E can be found. For coasting energies of around 300 kv, where most of the experiments were run, errors in k and $\frac{df}{dE}$ have relatively little effect on E, a 10% error in either causing approximately a 10 kv error in E. The values of E obtained in this way are consistent within estimated errors with those found from radius and field calculations (Fig. 5) but, as discussed above, are considered to be more accurate.

B. Radio frequency experiments.

1. Beam capture by one rf pulse.

This situation is indicated in Fig. 3. As long as the rate of frequency modulation is sufficiently low, electrons are captured whenever the turn on frequency of the rf oscillator is adjusted to the revolution frequency of the coasting electrons.

a. Threshold voltage for rf capture.

Particles with zero amplitude of phase oscillation gain the synchronous energy per turn V_s; with finite amplitudes, this is the average energy gain. The synchronous voltage can be calculated:

$$V_s = \frac{\frac{df}{dt}}{f\,\frac{df}{dE}}$$

where f, df/dt and df/dE are all measurable quantities, as described in section A. V_s can also be found independently by observing the threshold rf voltage for capture. A comparison of the two determinations of V_s should show agreement within the accuracy of the different measurments involved. The errors in the measured quantities are of order 10% except for f which can be read to a few kc. Results are presented in Table I. For this and the other quantitative experiments

TABLE I
Determination of rf threshold voltage.

Measurements	Calculated V_s	Measured threshold V_s
f 72.2 Mc		
$\frac{df}{dt}$ 16.1 $\frac{Kc}{\mu s}$	8.4v	8.8v
$\frac{df}{dE}$ 26.6 $\frac{Kc}{KV}$		

the electron coasting energy is 300 kv and k is 3.51. The target energy is 365 kv, the target radius is 50.3 cm, and the electron frequency at the target is 73.5 Mc. The good agreement is well inside experimental errors. The above experiment of course does not test the Symon-Sessler rf theory, but only experimental consistency.

b. Energy spread in a moving rf bucket.

An experimental estimate can be made of the range of energies accepted by a moving rf bucket and also the spread in energy of the coasting beam. This is done by observing the range of rf turn on frequency over which any beam can be captured. From the Δf, and df/dE, previously found, a ΔE is obtained. This ΔE of course includes both the energy width of the capturing bucket and the coasting beam.

The maximum spread of energy of particles in a moving bucket can be calculated using the SS theory:

$$\Delta E = y\sqrt{\frac{2fV}{\pi\, df/dE}}$$

where y is defined and graphed in SS. It is approximately equal to 2 (1- $\frac{V_s}{V}$).

The calculated energy spread in a bucket for different applied rf voltages is plotted in Fig. 6 against the experimentally determined spread, which includes both beam and bucket. The agreement is within experimental error, the calculated ΔE being about 15% higher then the measured. The plot indicates the energy spread in the beam is small, less than a kilovolt.

c. Beam capture with rf at injection.

As a side experiment, the starting rf oscillator frequency was changed to correspond to the electron revolution frequency at injection. Without the betatron pulses but using the beam expander, a good fraction of the injected beam was satisfactorily captured by the rf and accelerated over the oscillator frequency range of 38 to 48 Mc. Some beam was picked up even without the expander, which has also been true with betatron acceleration.

2. Phase displacement experiments.

Two experiments have been performed to test the phenomena of phase displacement predicted by the SS theory. The prediction is that an rf pulse which starts with a frequency below that of the coasting electrons and modulates through the coasting frequency should decrease the average energy of the coasting beam by just the average energy spread of the bucket, while capturing only a very few electrons in the process. The average energy spread of an rf bucket is given in SS as

$$\overline{\Delta E} = \frac{Af}{2\pi}$$

where A is the bucket area in W-α space. W equals $\int \frac{dE}{f}$ and α is the phase angle. A is given by

$$A = \frac{8\sqrt{\frac{2}{\pi}}\, V \alpha \sqrt{\frac{V_s}{V}}}{\sqrt{df/dt}}$$

where $\alpha\left(\frac{V_s}{V}\right)$, plotted in SS, is approximately equal to $\left(1-\frac{V_s}{V}\right)^2$.

Symon has calculated the expected distribution of particle energies after an rf bucket has swept through the coasting beam. Not all of the coasting particles get the decrease of energy $\overline{\Delta E}$; there is a considerable spread in energy. In cases of small $\frac{V_s}{V}$ the peak energy loss and the average energy loss are quite close. The relation between the two is, very approximately,

$$\frac{\Delta E_{PEAK}}{\overline{\Delta E}} \cong \frac{1}{2}\left[1+\frac{1}{\left(1-\frac{V_s}{V}\right)^2}\right].$$

a. Betatron detection experiment.

To test this phase displacement, one or more rf sweeps are made to operate on the beam coasting between the two betatron pulses, as in Fig. 3, and any energy shift is measured with the aid of the second betatron pulse. The situation is pictured in Fig. 7, where two identical rf pulses are used, each long enough to accelerate any captured electrons to just short of the target energy. 7a shows the second betatron pulse. In 7b the rf pulses are turned on with starting frequency above that of the coasting electrons, and do not affect the beam appreciably; it appears at the same time as without the rf pulses on. The apparent energy spread on the beam, seen by the second betatron pulse to be about 15 kv, is due not the inherent spread, which is less than a kilovolt, but to the different amplitudes of betatron oscillation present. In 7c the starting frequency of the rf pulses is adjusted down to the coasting frequency so that a large fraction of the beam is captured and accelerated to a higher energy and comes in early on the second betatron pulse. In 7d the starting frequency is moved below that of the coasting electrons. The rf captures only a

trace of beam. The uncaptured coasting beam, accelerated to the target by the second betatron pulse, hits the target later in time, so there has been a measurable decrease in energy of the coasting beam by the upward passage of the rf buckets through it. The peak energy loss, measured by observing the downward shift in the right hand edge of the pulse, is observably larger than the average loss. Experiments with different numbers of buckets indicate that the average and peak displacements are proportional to the number of buckets, although the pulse pattern changes shape considerably with additional sweeps.

A number of quantitative determinations have been made. Results for the most reliable set of runs made with two rf sweeps are presented below. The measured time shifts are estimated accurate to about 10%. The corresponding energy displacements are presented in Table II, along with the calculated displacements. The conditions are the same as for the threshold voltage measurement.

TABLE II.

Phase displacement by two rf buckets, using betatron detection. Conditions as in Table I.

RF volts, peak	$\frac{V_s}{V}$		Energy loss per rf sweep, kv.		
			Maximum	Average	Ratio
42.5	.196	Measured	7.6	6.2	1.23
		Calculated	9.9	7.4	1.35
28	.30	Measured	5.7	3.8	1.50
		Calculated	7.8	4.9	1.59

The measured and calculated displacements appear to be in rough quantitative agreement, the calculated values being consistently about 30% higher than the measured. The ratios between the maximum and average displacements are in

good agreement with the theory, as well as the variation of the displacements with rf voltage. The systematic 30% difference must still be considered within experimental error, because of all the 10% measurements involved, even though the measured and calculated threshold voltages checked closely.

b. Rf pick-up detection experiment.

Another method of detecting phase displacement is to use the rf pulses themselves to find energy shifts. With this method the second betatron pulse is not needed. The situation is pictured in Fig. 8. with two identical rf pulses. The rf sweeps are long enough to accelerate any captured electrons to the target, The beat frequency patterns of the rf pulses with a constant frequency generator are presented along with the photomultiplier beam pulses. In 8a the starting frequency of the rf is well above the coasting frequency and no beam is accelerated. In 8b the starting frequency has been moved down to be just slightly above the coasting frequency, and some beam is picked up by the second rf pulse, presumably because of slight disturbances caused by the first pulse. At a slightly lower frequency, in 8c, the first pulse picks up the beam. At a still lower turn on frequency, in 8d, the beam is captured not by the first pulse, but by the second, indicating the first pulse has phase displaced the coasting beam downward in energy to where it can be captured by the second pulse. The turn on frequency shift from capturing by the first pulse to capturing by the second is quite considerable, far more than any possible turn on frequency differences between the two pulses, or changes in frequency of the coasting beam from other causes. From a measurment of Δf, and knowing df/dE, a ΔE is found. This ΔE, from tuning for maximum picked up beam, can be anywhere from $\overline{\Delta E}$ to ΔE peak. As in the previous experiment, ΔE is proportional to the number of rf sweeps displacing the beam. The measured frequency shift is accurate to

about 10%. Results with three rf pulses, two displacing and one detecting, are presented in Table III, along with the calculated values.

TABLE III

Phase displacement by two rf buckets, using rf pick up detection. Conditions as in Table I, except that df/dt is 13 kc/μs instead of 16 kc/μs.

Rf volts, peak V	$\frac{V_s}{V}$		Energy loss per rf sweep, kv Maximum	Average
42.5	.155	Measured	8.0	
		Calculated	9.9	7.9
28	.245	Measured	6.2	
		Calculated	7.8	5.4

The measured displacements are consistent both with the calculated values and the measured values of the previous experiment, because of the uncertainty in what ΔE is being measured by this technique. The variation with voltage is almost exactly that of the calculated maximum displacements, however, indicating that the measured displacements may be closer to the maximum than to the average. If this is so, the results check the measurements of the previous experiment quite well.

3. Beam stacking tests.

Some qualitative tests of beam stacking have been performed. One of these is indicated in Fig. 9. The photograph is taken during the period of the second betatron pulse, and is similar to Fig. 7. The rf voltage is low, to keep the buckets small. In Fig. 9a, no rf pulses are present, in 9b there is one, in 9c two, 9d three, and 9e four. It is evident that the additional rf pulses are transferring more beam to the high energy, as expected. In Fig. 10, the situation is similar, only more pulses are used and the rf is again at maximum voltage. 10a shows no rf pulses, 10b one, 10c four, 10d seven, and 10e ten. Most of the beam is picked up by the first

pulse, and practically all by four pulses. The stacked beam is phase displaced downward by the successive rf pulses until some reaches the rf starting frequency, where it is captured and taken up to the top energy again. The beam stays pretty well contained between the frequency limits of the rf sweep, with a few particles displaced somewhat further down in energy.

The above group of experiments, we believe, offers fairly convincing evidence of the essential correctness of the Symon-Sessler rf theory, and the consequent possibility of stacking to obtain high intensities or large circulating beams.

We wish to acknowledge many fruitful discussions on the subject of these experiments with R. O. Haxby, D. W. Kerst, F. E. Mills and K. R. Symon, and many other members of the MURA technical staff.

FIGURE CAPTIONS

Fig. 1. Oscilloscope photograph of method of obtaining electrons coasting at an intermediate energy. Time scale 500 μsec/cm.

a. Betatron waveform, 3v/cm.

b. Portion of waveform used for acceleration, injection time indicated by a spike near peak of first pulse. 5v/cm.

c. Photomultiplier pulse from beam striking target after acceleration by second betatron pulse.

Fig. 2. Oscilloscope photographs of rf pulses.

a. Pulse from a diode detector on the rf gap. The time scale is 50 μsec/cm. The maximum voltage is about 45 volts.

b. Beat frequency patterns of the above rf pulse with a signal generator. The signal generator is set at 72.5, 73.0 and 73.5 Mc in the different traces.

c. and d. Detector signal and beat frequency pattern from a group of rf pulses. The time scale here is 200 μsec/cm.

Fig. 3. Photographs of a frequency modulated rf pulse operating on the coasting beam between the two betatron pulses. Time scale is 500 μsec/cm.

a. Betatron and rf pulses.

b. Photomultiplier pulses from beam striking target. The turn on rf frequency is tuned for beam capture at the coasting electron frequency. The rf is 14 volts peak.

c. As in b, only the rf is raised to 46 volts, capturing more beam.

d. As in c, only the turn on rf frequency is below the coasting electron frequency. Some beam is picked up as the rf sweeps through the coasting frequency, due to the growing rf bucket.

Fig. 4. Measured oscillator frequency as a function of time for an rf pulse.

Fig. 5. Calculated electron energy and revolution frequency as a function of radius.

Fig. 6. Plot of calculated energy spread in a bucket versus a measured energy spread. The latter includes both beam and bucket. The parameter $\frac{df}{dt}$ is not exactly the same at the different points, but varies from 14 to 17 $\frac{kc}{\mu s}$ with changing rf voltage. $\frac{df}{dE} = 26 \frac{kc}{kv}$. The applied rf voltage went from 11.5v to 46.4v, peak values. f is 72.2 Mc. The energy spread in the beam is seen to be under a kilovolt.

Fig. 7. Photograph showing phase displacement using betatron detection. The situation is similar to Fig. 3, with two identical rf sweeps, except the rf does not accelerate captured electrons all the way to the target. Rf is 45 volts, the time scale is 20 μsec/cm.

a. Second betatron pulse at 5v/cm.

b. Photomultiplier pulse of beam striking target with rf starting frequency above the electron coasting frequency.

c. Rf starting frequency tuned to coasting frequency, so most of the beam is rf accelerated to a higher energy and comes out early on the second betatron pulse.

d. Rf starting frequency below the coasting frequency. Only a little beam is captured and the rest is displaced later in time on the second betatron pulse.

Fig. 8. Photograph showing phase displacement using rf pick-up detection. Situation as in Fig. 3, with two identical rf pulses. Time scale is 100 μs/cm. Beat frequency patterns between the rf pulses and a constant frequency rf generator are shown along with the photomultiplier pulses.

Fig. 8a. Rf starting frequency well above the coasting frequency.

b. Rf starting frequency just slightly above the coasting frequency.

c. Rf starting frequency equals the coasting frequency and the beam is captured by the first pulse.

d. Rf starting frequency is below the coasting frequency and the beam is captured by the second pulse, indicating the first pulse has caused a decrease in energy of the coasting beam.

Fig. 9. Photograph demonstrating beam stacking. Situation is as in Fig. 7. Rf is 10 volts.

a. No rf pulses.

b. One rf pulse, capturing beam.

c. Two rf pulses identical to the one in b.

d. Three rf pulses.

e. Four rf pulses.

Fig. 10. Photograph showing beam stacking and phase displacement. Situation as in Fig. 7, with a time scale of 25 μsec/cm. Rf is 45 volts. The second betatron pulse has been delayed out to 5ms to permit a large number of rf pulses.

a. No rf pulses.

b. One rf pulse, capturing beam.

c. Four rf pulses, identical to the one in b.

d. Seven rf pulses.

e. Ten rf pulses.

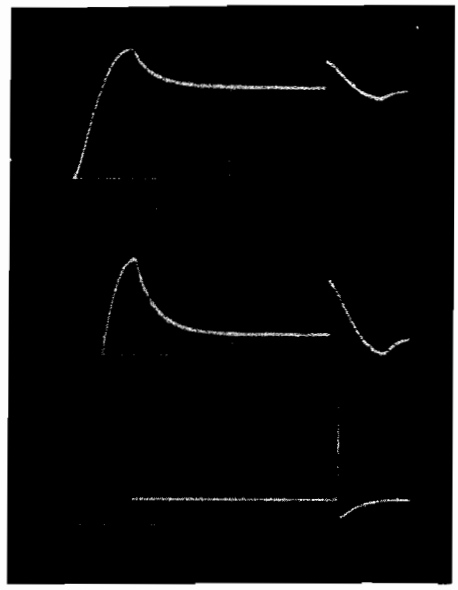

Fig. 1

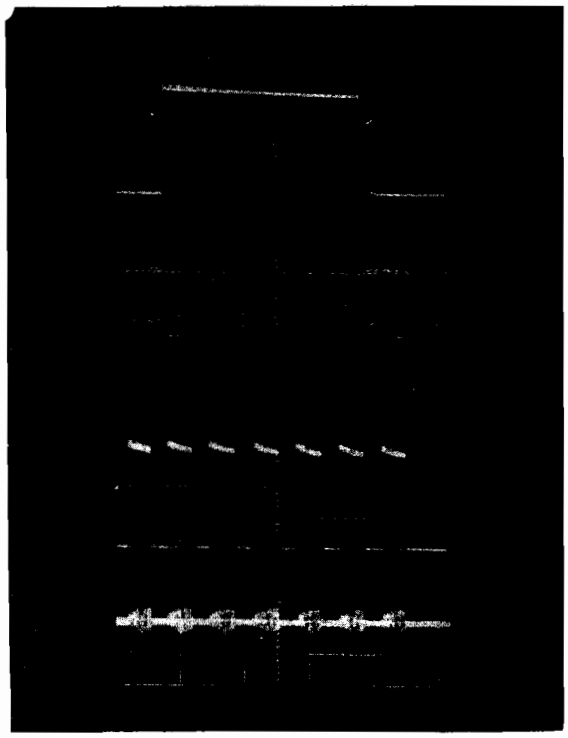

Fig. 2

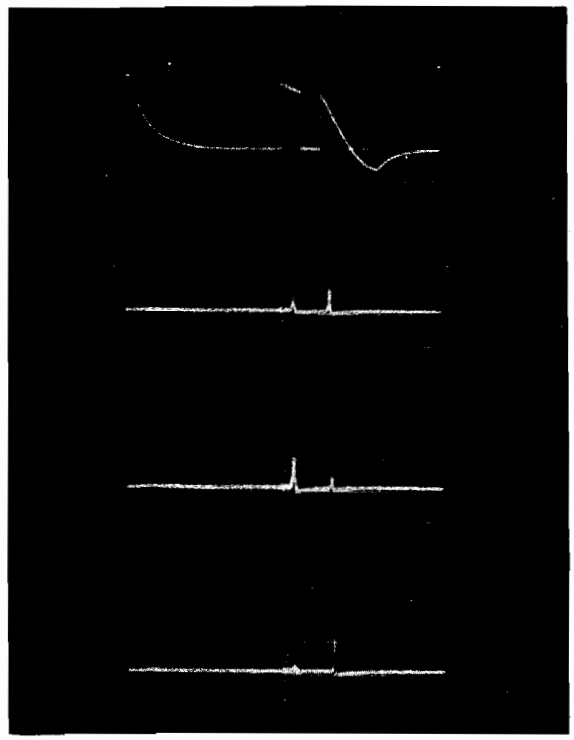

Fig. 3

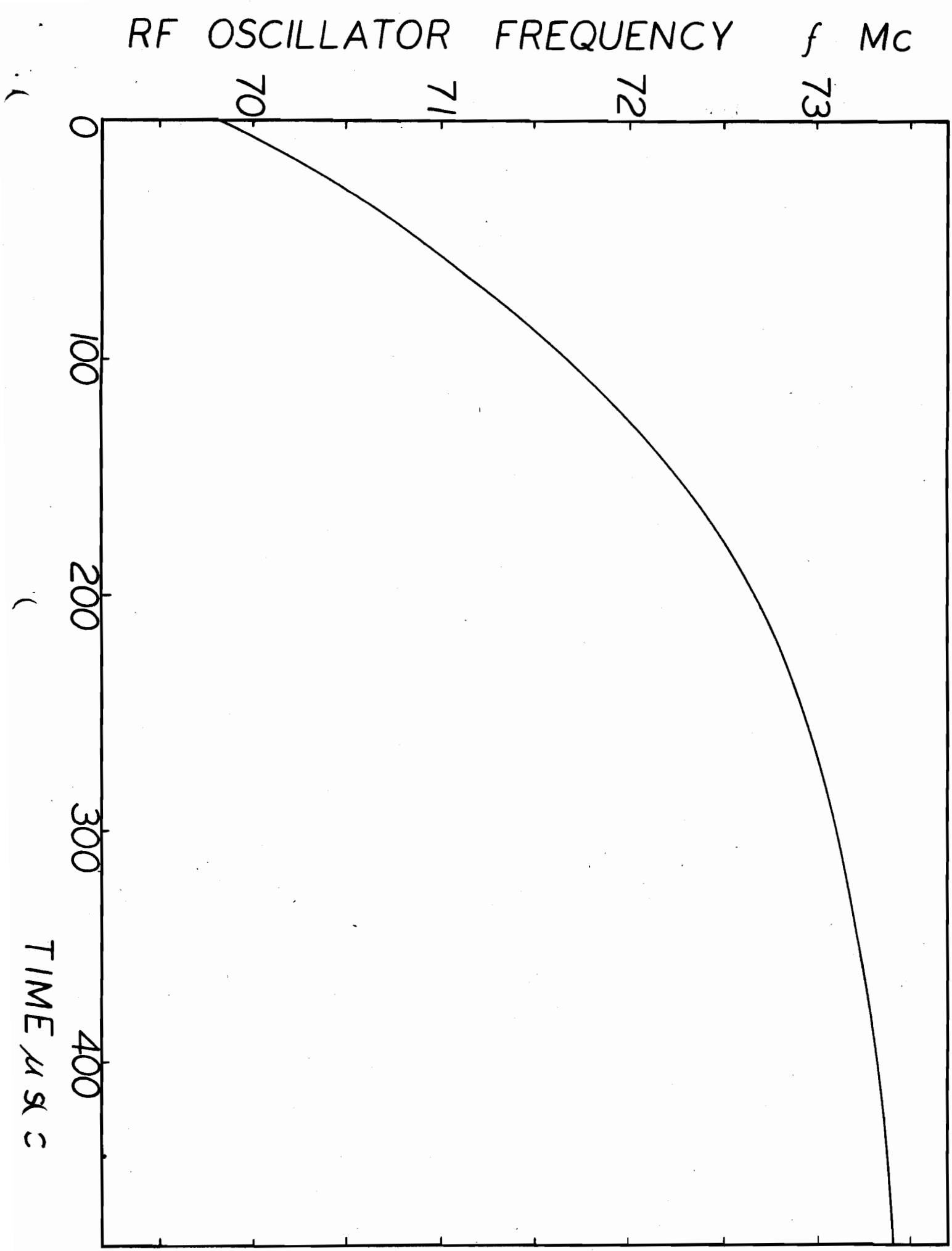
RF OSCILLATOR FREQUENCY f Mc
70
71
72
73
0
100
200
300
400
TIME μ SEC

Fig. 4

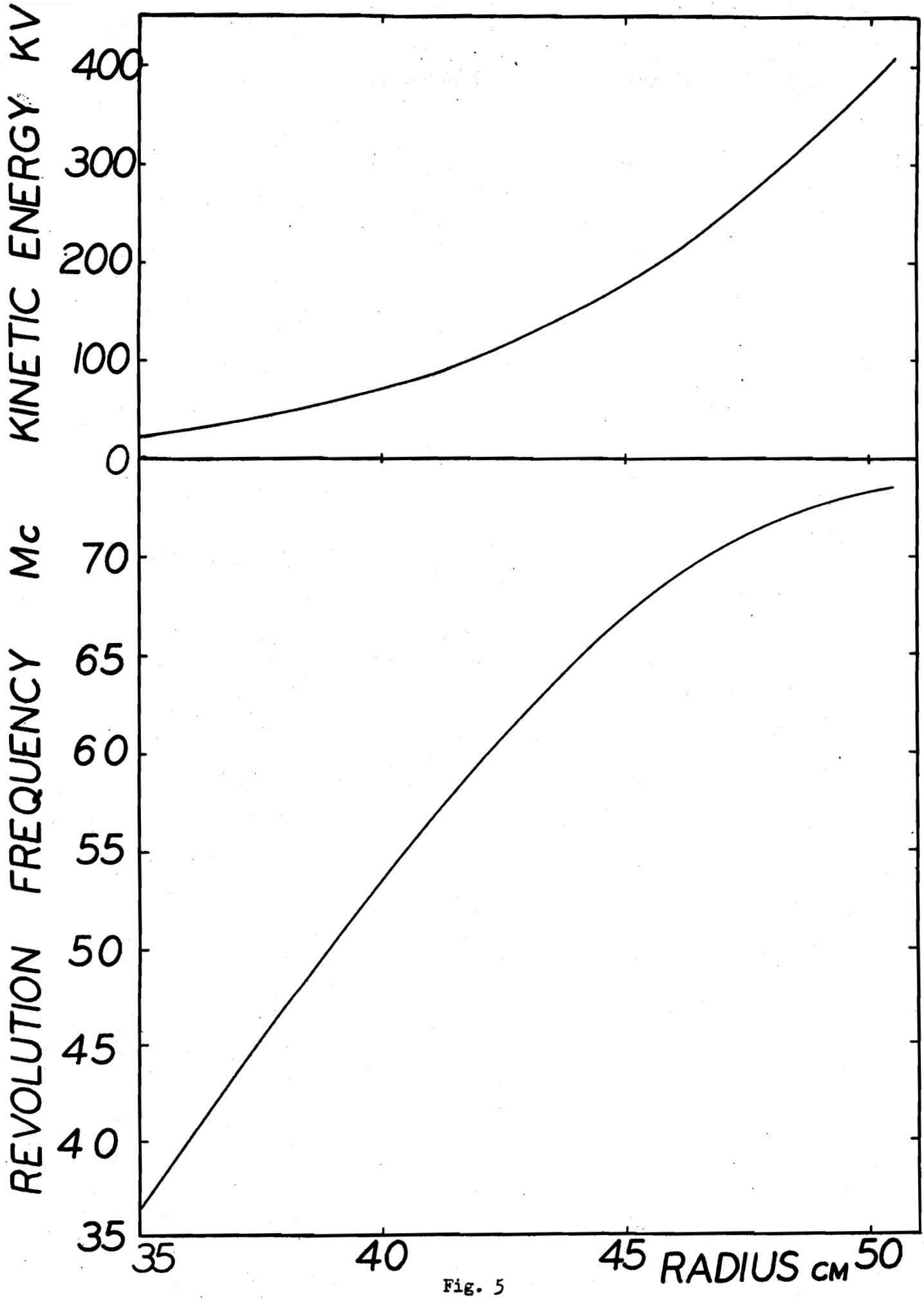
KINETIC ENERGY KV
400
300
200
100
0
REVOLUTION FREQUENCY Mc
70
65
60
55
50
45
40
35
35
40
45
50
RADIUS CM

Fig. 5

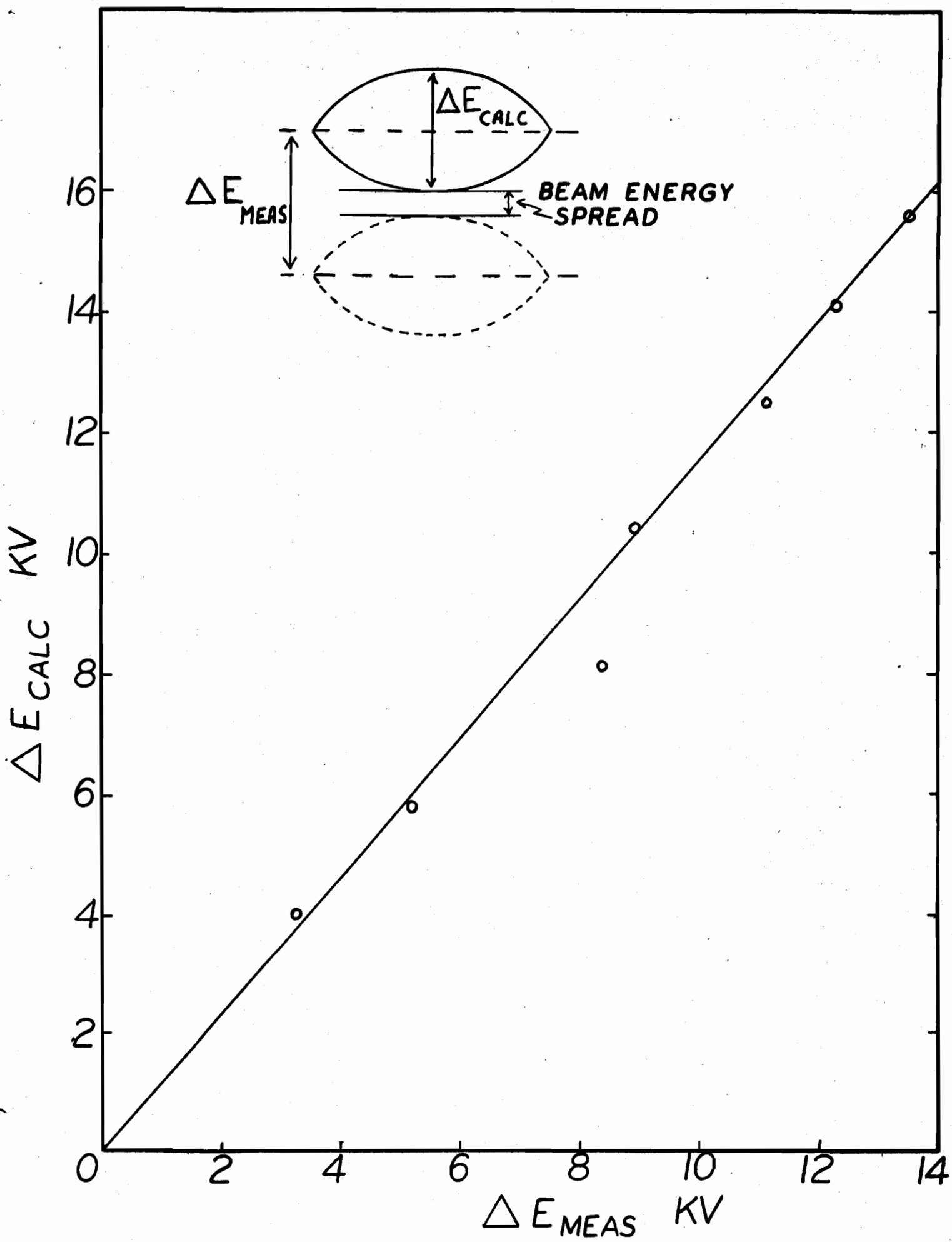
ΔE CALC
ΔE MEAS
BEAM ENERGY
SPREAD
16
14
12
10
8
6
4
2
0
2
4
6
8
10
12
14
Δ E CALC KV
Δ E MEAS KV

Fig. 6

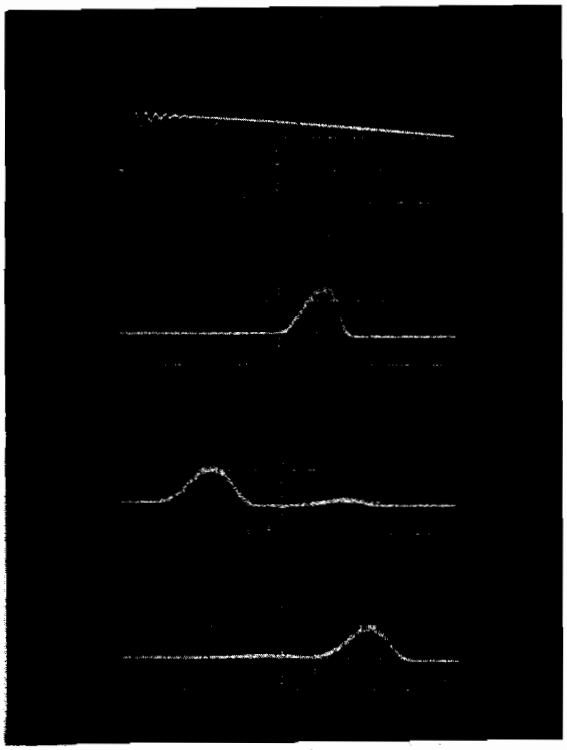

Fig. 7

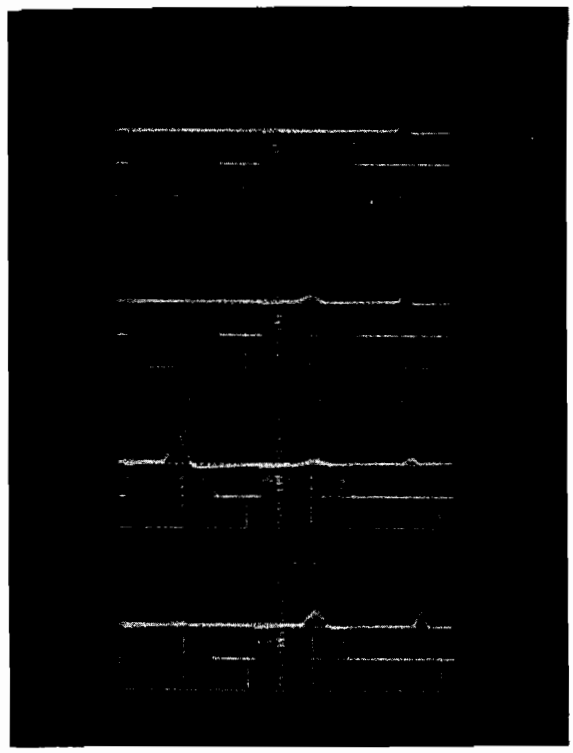

Fig. 8

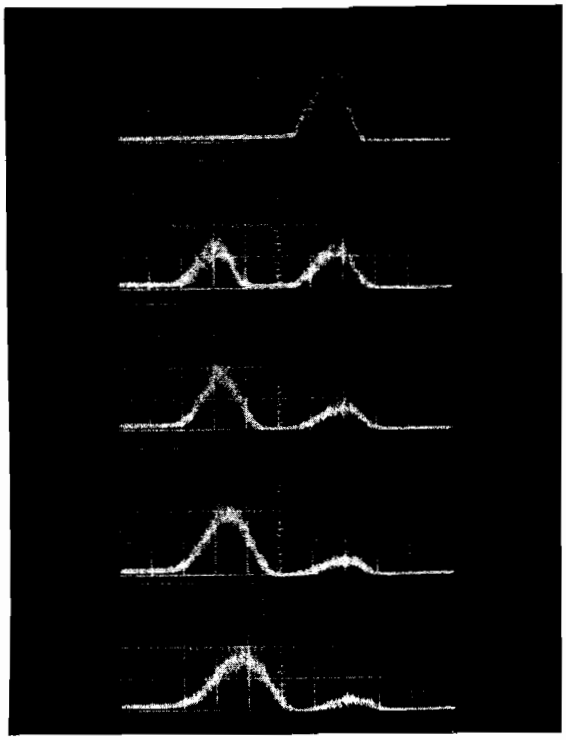

Fig. 9

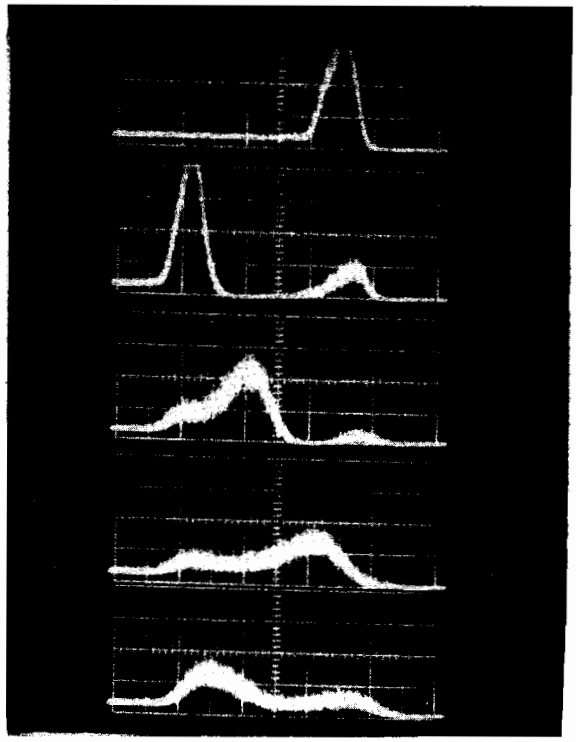

Fig. 10